A Computational Approach to Unravel Principles of Epithelial Morphogenesis

Chapter 4. Simulating early glandular epithelial cancer progression

4.1. Background

Epigenetic deregulation of cell activity is thought to be an important requirement in the preclonal phase of glandular epithelial cancer (Tlsty et al., 2004). What level of deregulation is required before the histology becomes abnormal? Can a mechanism of deregulation be inferred from the abnormal phenotype? To better understand causal linkages between mechanisms and phenotype in an in vitro setting, epithelial cells have been cultured in three-dimensional (3D) gels of extracellular matrix (ECM), such as collagen I or Matrigel®. When grown embedded in 3D culture, Madin-Darby canine kidney (MDCK) cells form identically structured acinar organoids enclosing a cell-free, fluid-filled lumen (O'Brien et al., 2002). Proliferation and apoptosis are essential features of the process. When manipulated or exposed to certain factors, the organoids and composing cells exhibit phenotypic features that are associated with pre-cancerous or cancerous tissues in vivo (Debnath et al., 2002). These culture models are thought to provide an appropriate physiological environment to study glandular epithelial morphogenesis and cancer progression.

From a systems modeling perspective, cell cultures are abstract, somewhat simplistic models of epithelial cells in vivo. They are constructed wet-lab models: a controllable, careful assemblage of laboratory materials and equipment, in which one component is alive. There is little direct overlap between measured in vitro phenotypic attributes and corresponding attributes of epithelial cells in vivo (Fig. 4.1). Nevertheless, the accumulated literature and the model's continued study attest that scientifically useful mappings exist between model and referent at

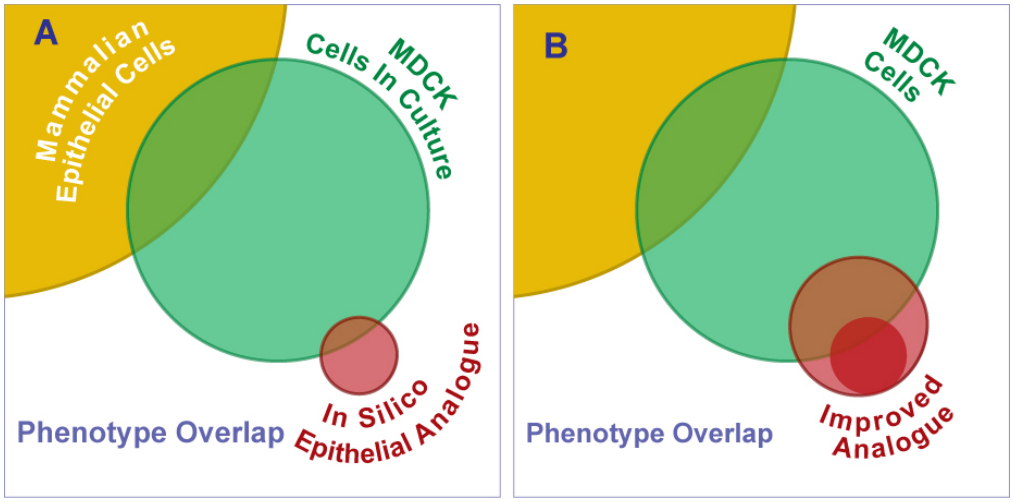

Figure 4.1. Phenotype overlap. MDCK cell cultures are studied because they are useful, abstract models of epithelial cells in humans, even though the two systems are fundamentally different in many ways. The shaded areas illustrate overlapping sets of phenotypic attributes. There is direct overlap of some systemic attributes of MDCK cultures and corresponding epithelial cell attributes in tissues. Overlap of cell and molecular level attributes is believed to be greater. An in silico analogue of the class described in the text is intended to have a similar relationship to MDCK cultures. It is a standalone, real system comprised of software components. The principles governing component interactions are axioms. Phenotypic attributes observed during execution are unique. Overlap (similarities) in phenotype between the in silico analogue and MDCK cultures are intended to reflect similarities (but not precise matches) in components, mechanisms, and operating principles. **A:** The first analogue is simple and abstract. It validates when a set of its attributes are acceptably similar to a targeted set of MDCK culture attributes (area of overlap). As is the case with MDCK cultures relative to epithelial cells in mammalian tissues, the analogue also has attributes that have no MDCK counterparts (non-overlapping area). **B:** Sequential, iterative refinement of the first analogue leads to an improved analogue. Its validation is achieved when a larger set of its attributes are judged similar to an expanded target set of MDCK attributes.

several levels, from genetic to systemic phenomena (Montesano et al., 1991; O'Brien et al., 2002; Martín-Belmonte et al., 2008). However, even though the in vitro cultures are orders of magnitude simpler than epithelial cells in a human tissue context, they still are complex systems that have proven challenging to understand.

We suggest that progress can be made in understanding epithelial cell behavior, phenotype, and mechanism, and the changes that occur during cancer progression by constructing and studying abstract analogues in software, where the system features at all levels (Fig. 4.2) can be modeled, fully explored, and understood. The envisioned software analogues will not be traditional analytical inductive models of data collected during study of cell cultures. Nor will their use be limited to modeling aspects of cells in culture (even though they will be quite capable of doing so). Both of these model uses are within the traditional domain of computational biology. Rather, the approach we have taken is conceptually different and is intended to be synergistic with the traditional methods. The envisioned analogues will be advanced examples of executable biology (Fisher and Henzinger, 2007; Hunt et al., 2008).

In a previous study (Grant et al., 2006), we presented a cell-mimetic analogue of the envisioned type, which validated for a small set of targeted MDCK attributes. Its growth characteristics and the types of stable structures formed mimicked those of MDCK cells in cultures. Eleven axiomatic operating principles, and six simulated cell actions, were adequate for validation. However, it failed to consistently produce cystic structures with a round, convex contour, a cardinal feature of normal in vitro phenotype which has not been considered in the earlier study.

Starting with the earlier analogue, we explored several analogue revision strategies to achieve the expanded attribute set. Because of the networked nature of axiom use, some changes intended to have one effect also had other, unintended, often abiotic consequences. One of our guidelines was to keep revisions parsimonious. We sought one new analogue having as few new

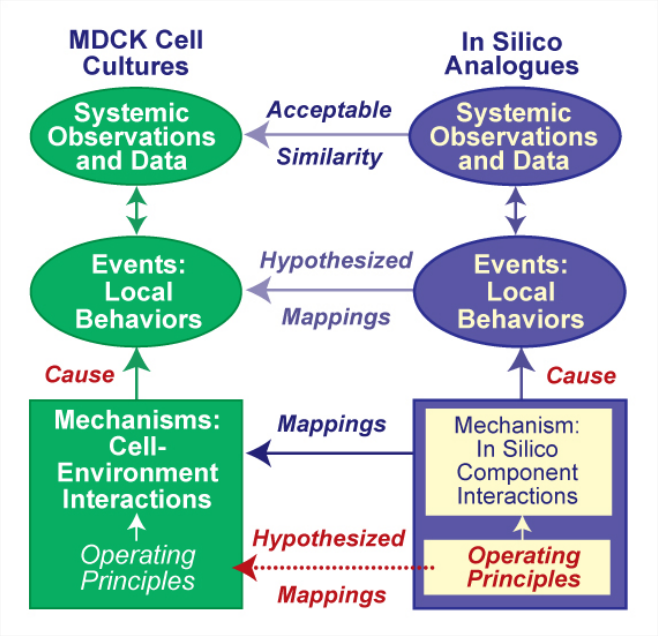

Figure 4.2. Relationships between in silico analogues, and MDCK cells in culture. To distinguish simulation components and characteristics from in vitro counterparts, we use small caps when referring to the former. An in silico analogue is comprised of autonomous CELL components interacting with adjacent CELLS and components of their environment. Interactions are governed by a set of axiomatic operating principles. For each circumstance a CELL can encounter, there is a corresponding axiom. A clear mapping exists between the in silico components (CELL states and environment components) and in vitro counterparts. Following execution, interacting components cause local and systemic behaviors. Measures of CELL and system behaviors (growth rates, structure type, etc.) are the in silico attributes. Validation occurs when a prespecified set of in silico attributes is measurably similar to a corresponding set of in vitro attributes. Upon validation, we can hypothesize that a semiquantitative mapping exists between in silico events and in vitro events, and that the set of in silico operating principles has a biological counterpart.

axioms as possible to achieve validation against the shape requirement, in addition to the original set of target attributes. For one, validation was achieved by addition of only one new cell action coupled with replacement of one axiom. Use of the new action enabled the improved in silico epithelial analogue (ISEA) to form stable cystic structures with smooth, convex margins similar to those observed normally in 3D epithelial cell culture.

We reasoned that if a mapping exists between ISEA's coarse-grained operating principles and the more complex epithelial cell counterparts, then selective disruption of ISEA's operation should exhibit cancer-like characteristics of in vitro epithelial cancer reconstruction models (Debnath and Brugge, 2005). We designed and implemented methods to selectively deregulate, at a controlled level of severity, simulated cell operation at the axiom level. We focused on two processes known to be critical for normal ISEA growth and stabilization. One process ended with an ISEA version of anoikis, a specific form of cell death due to extracellular matrix detachment. The other involved directed placement of a daughter cell, the ISEA's version of oriented cell division. A grading measure was developed and used to quantify changes in morphology.

Dysregulation of either "anoikis" or directed daughter cell placement, or both, led to manifest changes in ISEA phenotype that were reminiscent of dysplastic growth associated with in vitro cancer reconstruction and early glandular epithelial cancer progression in vivo. Consequently, we undertook a detailed analysis of the deregulations and their consequences. Varying the level of dysregulation led to morphologies that could be classified into groups using automated grading. Dysregulation of ISEA's anoikis process had a greater effect on overall phenotype. Simultaneous dysregulation of the two axioms had a nonadditive effect. Importantly, dysregulation of either process resulted in similar morphological outcomes, which could not be differentiated reliably without additional information on growth dynamics, with potentially significant implications for early cancer diagnosis based on histology. The results also provided an early lead on possible additional mechanisms to reconstruct, or revert, cancer-like phenotype in experimental and

therapeutic context. We expect future rounds of development and use will bear a viable platform to unravel operational basis of glandular epithelial morphogenesis and early cancer progression.

4.2. Methods

4.2.1. Modeling approach

Traditional inductive modeling and the approach used herein present different yet complementary approaches to exploring explanations of biological phenomena. Models of the former type are usually built by first analyzing data, creating a mapping between the envisioned system structure and components of the data, and then representing the generation of those data components with mathematical equations. Inductive analytical models test hypotheses about data. The method relies heavily on the researcher's knowledge combined with induction. When successful, it creates models that can extrapolate beyond the original data, making the method ideal for prediction. The class of models and methods described herein are different (Hunt et al., 2008). They are designed primarily to develop, test, and refine mechanistic explanations or hypotheses about biological phenomena. They are what Fisher and Henzinger (2007) have referred to as executable biology. For a specific referent system, we identify the perspective taken in the wet-lab along with the system aspects on which to focus, and then state the uses to which the model would be put. Next, we propose building blocks and their functions, along with assembly methods so that the components and assembled system map logically to wet-lab counterparts, as illustrated in Fig. 4.2. We refer to the in silico system as an analogue to help distinguish this class of models from traditional, inductive models. Analogues are executed and measured in the same way as their referents. Data accumulated during executions are compared against data taken from the referent. When an analogue fails validation, we revise; validate it against its predecessor (cross-model validation) and then against referent attributes. When satisfaction is achieved, a case can be made for each of the mappings in Fig. 4.2. The assembled components and their operating methods stand as a hypothesis: these mechanisms will produce

targeted characteristics. Execution tests that hypothesis. The methods provide for establishment of plausible reductive hierarchies between lower level mechanisms and higher-level phenomena by growing useful, more detailed in silico analogues from a predecessor.

4.2.2. Discrete event simulations using agents

The in silico epithelial analogue (ISEA) is based on the methods and principles of agent-based modeling (Grimm et al., 2005) and discrete event simulation (Law and Kelton, 2000; Zeigler et al., 2000). In agent-based modeling, a system is comprised of quasi-autonomous, decision-making entities called agents. An agent follows a set of rules that governs its actions and interactions with other system components. Agent-based modeling facilitates creating systemic behaviors and attributes that arise from the purposeful interactions of components. The resulting models have advantages when attempting to understand and simulate phenomena produced by systems of interacting components. We used quasi-autonomous agents to represent epithelial cells. We also employed quasi-autonomous components outside of the simulated biology for experimentation and analysis (Fig. 4.3), but still within the computational framework. In discrete event simulations, system operation is represented as a temporal sequence of events, occurring within discrete time intervals. System state evolves during those discrete time intervals. Using such methods facilitated encapsulating system operations and conceptualizing complex dynamics. The methods provided a rigorous formalism for managing modularity and hierarchy in space and time. From a simulation perspective, activities such as cell division, death, and polarization could be represented as being discrete. Stochasticity, which is natural to both agent-based modeling and discrete event simulations, was introduced mostly in the form of probabilistic parameters that regulated agent actions and execution order.

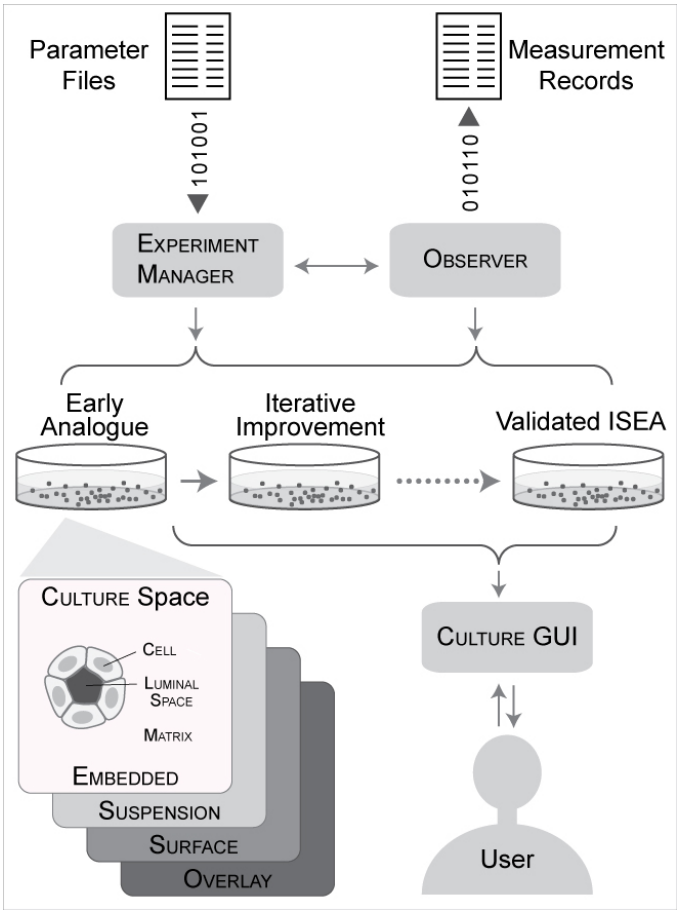

Figure 4.3. ISEA components and system architecture. The system consists of four CULTURE spaces and the framework components needed to support in silico experimentation and analysis. The focus is on simulations in EMBEDDED CULTURE. A CULTURE maps to a single MDCK cell culture. It is a composite of three object types: CELLS, MATRIX, and FREE SPACE. A hexagonal grid provides the CULTURE space within which components interact. CELLS are quasi-autonomous agents whose actions are driven by their internal logic and the set of axiomatic operating principles in Fig. 4.4. The ISEA that validated against the targeted attributes was preceded by earlier analogues. The framework supports ongoing iterative refinement. EXPERIMENT MANAGER is the agent that controls each experiment. It prepares parameter files, manages experiment execution, and processes experimental data for analysis and summary. OBSERVER automatically conducts and records measurements made on CULTURE. CULTURE GUI provides a graphical interface to visualize and interactively probe CULTURE during execution.

4.2.3. ISEA and the experimentation framework

To clearly distinguish ISEA components and processes from their in vitro counterparts, hereafter we use small caps when referring the former. EXPERIMENT MANAGER, OBSERVER, and CULTURE graphical user interface (GUI) enable semi-automated experimentation and analysis. They can accommodate non-specific CELL types, akin to how generic, common laboratory equipment and apparatus are used for cultures of different cell types or lines. EXPERIMENT MANAGER, the top-level system component, provides experiment protocol functions and specifications. The specifications define the mode of experimentation and the system's parameter vector. Experiments can be conducted in default, visual, or batch modes. An experiment in default mode is simply a single execution. In visual mode, a CULTURE GUI is created and the visualization console launched. Using the visual controller, the user can start or pause a simulation, as well as access current states of objects at CULTURE grid positions during simulation. Batch mode enables automatic construction and execution of multiple experiments, as well as processing and analysis of recorded measurements. EXPERIMENT MANAGER has user-defined specifications to delimit the parameter space from which individual CULTURE parameter files are generated. Once parameter files are generated, EXPERIMENT MANAGER automatically executes a batch of experiments, each corresponding to a different parameter file. Repetitions are executed sequentially. After completion of all experiments, basic analytic operations are used to collect and summarize data.

OBSERVER is responsible primarily for recording measurements. It is created and assigned to a CULTURE when it is initialized. OBSERVER is stepped and its probe method called at the end of every simulation cycle. The probe method scans the CULTURE internals and performs measurements, the results of which are recorded as time series vectors. At simulation's end, data are written to files for analytic processing by EXPERIMENT MANAGER. OBSERVER also implements a simple method to automatically record the execution count of individual CELL

axioms. Using CULTURE GUI functionalities, OBSERVER can capture and store time-lapse CULTURE images for post-processing.

4.2.4. In silico culture components

A CULTURE is an agent that maps abstractly to the MDCK cell culture within one well of a multi-well culture plate. It has basic simulation components as well as base methods that are called automatically at the simulation's start and end. A CULTURE uses a standard two-dimensional (2D) hexagonal grid to provide the space in which its objects reside. The grid represents an arbitrary cross-section through a 3D MDCK cell culture. The grid has toroidal topologies. The start function is used to initialize the grid, CELLS, MATRIX, and FREE SPACE (discussed below) and to schedule initial CELL events on a master event schedule. Simulation starts following completion of the CULTURE start function. As execution advances, the event schedule is stepped for a number of simulation cycles or until a stop signal is produced. Simulation time is advanced discretely, and is maintained by the schedule. Ordering of events within the same simulation cycle is pseudo-random. Within a simulation cycle, each CELL in pseudo-random order is given an opportunity to interact with adjacent objects in its environment. Having objects update pseudo-randomly simulates the parallel operation of cells in culture and the nondeterminism fundamental to living systems, while building in a controllable degree of uncertainty. At the end of a simulation, the CULTURE finish function is executed to close remaining open files and clear the system.

Discrete objects with eponymous names represent the essential cell culture components: CELLS, MATRIX, and FREE SPACE. MATRIX and FREE SPACE are passive objects that map to units of extracellular matrix (ECM) and matrix-free material. A MATRIX object maps to a cell-sized volume of ECM. For simplicity, MATRIX represents any media containing sufficient ECM to which MDCK cells can attach. For the traits targeted, no distinction was needed for differential physical ECM characteristics, such as stiffness, density, and viscoelasticity. A FREE SPACE object

maps to a similarly sized volume of material that is essentially free of cells and matrix elements. FREE SPACE also maps to luminal space and non-matrix material in pockets enclosed by cells. The latter are called LUMINAL SPACE when distinction from FREE SPACE is useful.

CELLS are quasi-autonomous agents. They use the axiomatic operating principles and decision logic illustrated in Fig. 4.4 to interact with components in their local environment. Every CELL has the same step function in which an assessment of its environment is made and a call is made for an appropriate action. The step function is scheduled each simulation cycle. A set of CELL axioms, discussed below, determines CELL action. A CELL selects just one axiom and completes its corresponding action during each simulation cycle.

4.2.5. CELL operating principles

An agent must have rules and protocols for interacting with adjacent components. The operating premise illustrated in Fig. 4.2 is that the same is true for cells in culture; what can be described as rules and protocols are emergent properties of the cell's expressed genetics and ongoing biochemistry. An agent also needs a set of action options. A key engineering task is to invent a set of rules that will guide all CELL actions in all possible situations. The set that enables validation becomes the CELL's operating principles. One rule in isolation, even an apparently good one, cannot be an in silico operating principle because an agent using it alone (in combination with random actions when the rule does not apply), will, upon execution, not achieve prespecified, targeted attributes. Rules can take any form. We elected to have all rules take the form of axioms. We use the term axiom to reinforce that our computational model is a mathematical, formal system and that analogue execution is a form of deduction from the original axioms or assumptions explicitly programmed into the model. An axiom specifies a precondition and corresponding action. We specified what we judged to be a minimal set of action options: replace an adjacent non-CELL object with a CELL copy, DIE (vanish) and leave behind a LUMINAL SPACE, create MATRIX, destroy an adjacent non-CELL object and move to that location leaving

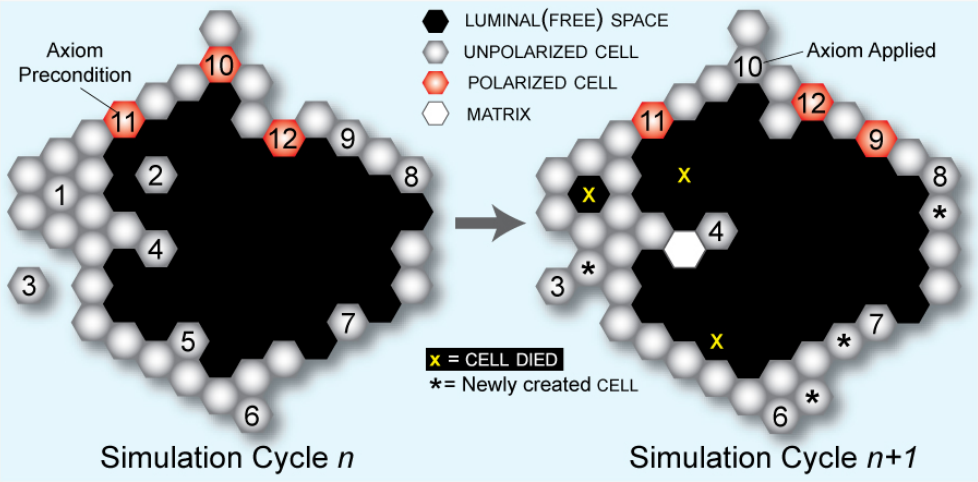

Figure 4.4. The twelve ISEA axiomatic operating principles. 2D space and all objects within are hexagonally discretized. Simulation time advances in steps corresponding to simulation cycles. Each simulation cycle maps to an identical interval of wet-lab time. During a simulation cycle, every CELL, in a pseudo-random order, decides what action to take based on its internal state (POLARIZED or UNPOLARIZED) and the composition of its adjacent neighborhood. A set of axioms determines what action is taken for each possible neighborhood configurations. Objects represented: POLARIZED CELL (red), UNPOLARIZED CELL (gray), MATRIX (white), and LUMINAL SPACE (black). To the left, selected decision-making CELLS at the start of simulation cycle *n* are numbered to indicate each of twelve axiomatic preconditions being satisfied. For purpose of this illustration, the unnumbered CELLS are inactive. To the right, the system at the start of simulation cycle *n* + 1 shows the consequences of applying all twelve axioms. Axiom 1: if all neighbors are CELLS (precondition), then DIE (delete self) and leave behind a luminal space (action). Axiom 2: if all neighbors are LUMINAL SPACE, then DIE and leave behind a LUMINAL SPACE. Axiom 3: if all neighbors are matrix, then replace a randomly selected MATRIX with a CELL copy. Axiom 4: if there are LUMINAL SPACE and one CELL, then add MATRIX between self and the adjoining CELL. Axiom 5: if there are at least two CELLS and a LUMINAL SPACE, but no MATRIX, then DIE and leave behind a LUMINAL SPACE. Axiom 6: if there are at least one CELL and a MATRIX, then create a CELL copy and replace an adjoining MATRIX that maximizes its number of CELL neighbors. Axiom 7: if there are at least two LUMINAL SPACES and a MATRIX, then create a CELL copy and replace any LUMINAL SPACE that adjoins MATRIX. Axiom 8: if there are two adjacent LUMINAL SPACES, a MATRIX, and at least one CELL, then create a CELL copy and replace any LUMINAL SPACE that adjoins MATRIX and LUMINAL SPACE. Axiom 9: if the POLARIZING precondition is met (the two CELL neighbors are separated on one side by MATRIX and on the other side by LUMINAL SPACE, then POLARIZE. Axiom 10: if the POLARIZED CELL has noncontiguous MATRIX neighbors, revert to NONPOLARIZED state. Axiom 11: if the POLARIZED CELL has a single MATRIX neighbor, then the POLARIZED CELL deletes the adjacent MATRIX, moves to its location, and leaves behind a LUMINAL SPACE. Axiom 12: if none of the preceding preconditions has been met, do nothing; CELL mandates achieved.

behind a LUMINAL SPACE, POLARIZE, DEPOLARIZE, and do nothing. For any precondition, only one action was executed. Of course, if we discretize space differently, the preconditions would be different, as would the axioms. However, the key behaviors and endpoints would be expected to be essentially the same.

The earlier axioms developed by Grant et al. (2006) enabled the analogue to validate for a set of basic MDCK cell culture attributes. Unlike its referent, the model frequently produced highly irregular, abiotic structures. We revised the axioms to enable ISEA to consistently develop CYSTS having roundish, convex shapes, a cardinal feature of a normal in vitro epithelial cyst. Note that a regular hexagon in a hexagonally discretized space maps to a circle in continuous space. Figure 4.4 describes and shows use of all 12 ISEA axioms. Axioms 1–10 were carried forward from (Grant et al., 2006). ISEA variants that were more elaborate also enabled ISEA variants to achieve the targeted attributes, but they were rejected because we strove to adhere to the guideline of parsimony. The preconditions correspond to a CELL'S neighborhood configurations. During each simulation cycle, every CELL uses its logic to select and carry out an action specified by one of the axioms when that axiom's precondition is met. CELLS act to establish and maintain differentiated contacts with all three object types and that process corresponds abstractly to the three surfaces mandate (O'Brien et al., 2002). An UNPOLARIZED state indicates that the CELL'S three surfaces mandate has not been achieved.

We considered and explored adding and using limited details about the axis of POLARIZATION. A CELL, following one of its action options, acquiring CELL neighbor or prior to creating a copy, for example, could assign itself a vectorial axis of POLARIZATION. Thereafter, an axiomatic precondition could include reference to the direction of POLARIZATION combined with neighborhood information. However, other analogues explored, including ISEA, achieved the targeted attributes without that added detail. Adhering to the parsimony guideline, we excluded POLARIZATION details because they were not needed to achieve the attributes targeted, but they

can be added easily when the need arises. Axiom 8 requires a CELL to be aware of the positions of its neighboring objects relative to each other and itself. A higher resolution mechanism that would be exchangeable for Axiom 8 could include having and using an axis of POLARIZATION.

4.2.6. Operational disruption of ISEA CELL axioms

Following implementation (and validation) of the revised axiomatic operating principles, our next task was to add a mechanism to disrupt the operation of individual CELL axioms selectively. We added a set of parameters, one per axiom, which controlled the probability of the decision-making CELL electing to follow the axiom when its precondition applies. The parameter values ranged from 0 to 1 inclusively. A parameter value = 1 corresponded to 100% adherence to the axiom. Setting the parameter to zero completely blocked execution of the prescribed action and, if specified, dictated an alternate action. At its decision point, each CELL drew a pseudo-random number (PRN) from the standard uniform distribution. The prescribed action was followed only when the PRN was ≤ the probability threshold set for the corresponding parameter.

Following exploratory simulations that considered many options, we specified alternative actions that mapped to plausible in vitro cell actions in a deregulated state. Axioms 1, 2, and 5 governed CELL DEATH; a reasonable alternative was to resist DEATH and remain ALIVE (i.e., do nothing). Axiom 3 dictated random placement of a CELL copy; its alternate action was to do nothing and thus prevent REPLICATION. We also assigned the alternate action of 'do nothing' to Axiom 4 (MATRIX production). Several dysregulated action options were available to Axiom 6 (ORIENTED CELL DIVISION). One was to do nothing, effectively suppressing CELL DIVISION. Another was undirected CELL DIVISION, placing the CELL copy in a random direction without regard for the number of CELL neighbors. We used the latter because adequate, supportive biological information was available. Axiom 7, which dictated CELL DIVISION, had available the same alternative action options. Axiom 8 (CELL DIVISION or POLARIZATION) had many plausible options. One was preventing CELL DIVISION; another, as above, was to allow the CELL to place a

copy of itself in any available location. Yet, another option was to enable POLARIZATION. The preconditions prescribing CELL DIVISION or POLARIZATION also could be swapped. The remaining axioms, Axioms 9-12, posed a similar problem of having many plausible action options. Because no experimental information was available to narrow the options, we elected to defer investigation of those axioms until more information becomes available.

4.2.7. Design of simulation experiments

The following describes a standard EMBEDDED CELL CULTURE design and its execution. First, the top-level system component, EXPERIMENT MANAGER, was initialized. Next, EXPERIMENT MANAGER created a new CULTURE and filled it with MATRIX. CULTURE width and height were set to 100. CULTURE initialized a PRN generator with a seed set to the system's clock; a new seed was used to initialize the CULTURE'S PRN generator at the start of each simulation. Every CELL maintained its own PRN generator. Pseudo-random seeds were generated from the CULTURE'S PRN generator to initialize those used by CELLS. A single CELL was placed at the center of the CULTURE grid to start simulation. Each simulation experiment comprised 100 Monte Carlo (MC) runs. Each MC run was executed for 50 simulation cycles. A new CULTURE was created for each repetition.

4.2.8. Specification and use of morphology index

The morphology index, *M*, weighs three basic features of MULTICELL morphology: local EXTRACELLULAR arrangement, *E*, structural discontinuity, *D*, and a structure's overall shape, *S*. For each CELL, the algorithm computes a numerical score based its neighborhood arrangement. An ideal arrangement corresponds to the Axiom 12 precondition. Higher scores are assigned to neighborhood configurations that deviate from that ideal. The collective EXTRACELLULAR arrangement score, *E*, is the mean of individual CELL scores. A CLUSTER is structurally continuous so long as it remains one connected body of CELLS and FREE (or LUMINAL) SPACE.

When structural continuity is broken, two or more CLUSTERS are formed. The structural discontinuity algorithm computes the number of disconnected bodies; that number translates to *D*. The shape profile algorithm takes into consideration a structure's overall 2D shape in hexagonal space and computes a score, *S*, which increases as shape becomes irregular or deviates from the ideal shape, a regular hexagon (a regular hexagon in hexagonal space maps to a circle in continuous space). The value of the morphology index becomes $M = E + D + S$. The maximum values of *E*, *D*, and *S* have been set to 3, 2, and 1 respectively, reflecting their assigned relative weights. The final morphology index value ranges from 1 (an ideal CYST) to 6 (disorganized). Lower scores are assigned to configurations that are more organized and roundish with a single LUMEN. A detailed description of the measure and algorithms are provided in Appendix.

4.3. Results

4.3.1. Validation against normal 3D embedded cell culture traits

We implemented a common framework and components (Fig. 4.3), some derived from the earlier analogue (Grant et al., 2006). Having a new general framework was needed in part to reduce unnecessary, cross-model redundancies between different candidate CELLS during analogue refinement, and facilitate an iterative model refinement process capable of automated cross-model validation. As done in (Grant et al., 2006), we validated the revised ISEA for all four, growth conditions: monolayer, overlay, suspension, and embedded cultures. Validation results for monolayer and suspension CULTURES were identical to those in (Grant et al., 2006). Results for overlay cultures were closer in appearance to in vitro observations (not shown). Marked differences were observed for the EMBEDDED CULTURE condition. That CULTURE condition is focus hereafter.

At the start of an EMBEDDED CULTURE simulation, a single CELL was placed in CULTURE space, surrounded by only MATRIX. As a simulation progressed, the CELL underwent repeated

rounds of CELL REPLICATION, followed by the formation of LUMINAL SPACE and an increase in CELL number and CYST diameter. The central LUMINAL SPACE grew as CELLS in the inner region DIED or moved out. The growth dynamics and final phenotype were similar to those observed for MDCK cells (Fig. 4.5A). The EMBEDDED CULTURE always formed stable CYSTS bordered by POLARIZED CELLS (Fig. 4.5B), and ISEA consistently produced CYSTS with a roundish, convex shape with smooth margins. During an occasional simulation, because of their changing, local environment one or more CYST surface CELLS failed to POLARIZE or DIE before the simulation ended. Such events prevented the local rounding out process that a POLARIZED CELL can undertake, preventing a few structures from stabilizing within 50 simulation cycles.

4.3.2. New capabilities for simulating epigenetic deregulation of cell processes

Following validation, we preceded with experiments to simulate inducement and progression of in vitro cell phenotypes that mimic early, preclonal stages of carcinogenesis. The progression involves alterations in tissue organization and morphology but low genetic changes (Tlsty et al., 2004). The experiments were motivated by questions such as these: what happens when normal cell operation and its regulation become faulty? To what extent can individual cell activities be disrupted separately and together, and still maintain an apparently normal phenotype? What visible changes accompany relaxation of tight control of a cell-level process? Can the operational cause of the changes be predicted from histological morphology? To obtain answers for ISEA, we conducted experiments in which the probability (p) of proper axiom operation was varied from 1 to 0. When proper operation was not followed, alternate, dysregulated actions were used. From an operational standpoint, having $p = 0$ represents a permanent change in the CELL'S operating principles throughout the simulation. A nonzero value below 1.0 specifies a reversible change in the CELL'S operation. It can be viewed either as the probability of the CELL behaving properly at any point in time, or the approximate percentage of time that the CELL acts normal (i.e., strictly adheres to the axiomatic operating principles illustrated in Fig. 4.4) during

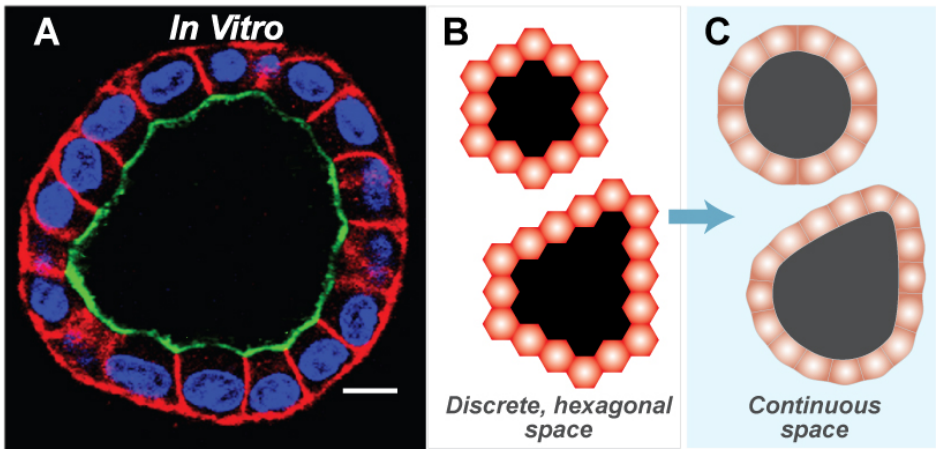

Figure 4.5. MDCK and simulated cysts. (A) MDCK cells grown in 3D extracellular matrix form lumen-enclosing cystic structures surrounded by a layer of polarized cells. Cells composing the cysts maintain three surfaces: apical (red), basal and lateral (green). Note the roundish contour typical of MDCK cysts. For growth and staining details, see Yu et al. (2005). Bar: ~10 µm. (B) Representative, stable ISEA CYSTS. CELLS in EMBEDDED condition produced stable, cystic structures enclosing LUMINAL SPACE; all CELLS were POLARIZED (red). CYSTS had convex shapes. (C) This illustration shows that convex polygonal CYSTS in discretized 2D hexagonal space map to a roundish structures in continuous 2D space. Because such a mapping provides no added scientific or mechanistic information, subsequent ISEA structures are shown as they appeared at simulation's end in 2D hexagonal space.

simulation. Individual CELLS decide to act normal (or not) independent of one another each simulation cycle, so CELLS can exhibit different behaviors (normal vs dysregulated) during a simulation cycle. With $p < 1$, a CELL can switch between the two behaviors multiple times during a simulation. It is a stochastic process having the Markov property: future changes in the CELL'S behavior occur probabilistically, independent of its history.

We focused on Axioms 5 and 6. Axioms 2, 3, 4, and 7, were not essential to normal (i.e., validated) CYST formation in EMBEDDED CULTURE (but they were needed for other simulated culture conditions), and were very infrequently used. Consequently, they were excluded from this investigation. As described in Methods, selecting an alternate action for disrupted Axioms 8–11 is not straightforward. Consequently, we elected not to pursue disruption of those axioms until further insight from wet-lab studies becomes available to narrow options. Disrupting Axiom 1 was straightforward but the outcomes (not shown) offered no significant insight: CELL CLUSTERS either developed normally into CYSTS ($p > 0$) or grew unchecked as a homogenous mass ($p = 0$). We expected that outcome because Axiom 1 is required for LUMINAL SPACE creation but becomes nonessential as soon as the nascent LUMINAL SPACE is formed. Axioms 5 and 6 were essential to CYST formation in EMBEDDED CULTURE. Axiom 5 dictates ANOIKIS (in silico counterpart to anoikis, a form of cell death), and is the most frequently used CELL DEATH axiom during CULTURE growth. Axiom 6 dictates oriented CELL DIVISION; the action requires making a CELL copy and placing it selectively. That process accounts for most of the CELL DIVISION events in the simulations. Their biological counterparts are centrally implicated in epithelial morphogenesis and carcinogenesis.

To aid investigation, we developed and used a morphology index to automatically quantify ISEA structure morphology. The algorithm analyzed and scored features of MULTICELL structures. The measure weighed three characteristics: local EXTRACELLULAR arrangement, structural continuity, and the overall shape. The index values ranged from 1 to 6. Higher values

indicated a more disorganized state. Lower scores were assigned when the overall shape was convex, and all CELLS were POLARIZED. The measure was calibrated for ISEAs, but could be generalized for other model types.

4.3.3. Dysregulation of Axiom 5 caused LUMEN filling

When cultured within 3D ECM, normal epithelial cells typically proliferate and organize into hollow spheroids, a process that recapitulates certain structural features of a glandular epithelium, such as the presence of a central, hollow lumen. In MDCK and some mammary cell cultures, apoptosis contributes centrally to lumen formation: cells in the inner region of the developing structure undergo anoikis upon loss of direct matrix contact (Boudreau et al., 1995). Blocking anoikis in vitro has been shown to cause lumen filling, which resembles a characteristic of most glandular epithelial cancers (Debnath et al., 2002). If ISEA's operating principles have cell culture counterparts, then simulation results should exhibit (predict) LUMEN filling when ANOIKIS is compromised. We simulated the condition by disrupting Axiom 5 use, which allowed CELLS lacking MATRIX contact (e.g., enclosed in the CYST LUMINAL SPACE) to evade DEATH for one or more simulation cycles. With nonzero $p < 1$, ANOIKIS was disrupted transiently, not permanently. In simulations with Axiom 5's $p = 0$, CELLS were essentially immune from DEATH on MATRIX detachment except when completely enclosed by other CELLS (Axiom 1). ANOIKIS dysregulation caused aberrant growth morphology (Fig. 4.6A), and changed CELL DEATH and DIVISION activity patterns.

For $p < 1$, mean ISEA CULTURE growth rates increased nonlinearly with increasing dysregulation. As evident in Fig. 4.7A, CULTURE growth became unchecked as CELLS evaded ANOIKIS more frequently. Growth became nonlinear at the lowest p values. CULTURE morphology also exhibited changes (Fig. 4.7B), becoming more aberrant with increased dysregulation. However, dysregulation had only a limited impact on morphology index during the early proliferative stage of ≤ 5 simulation cycles. Thereafter, values either decreased or

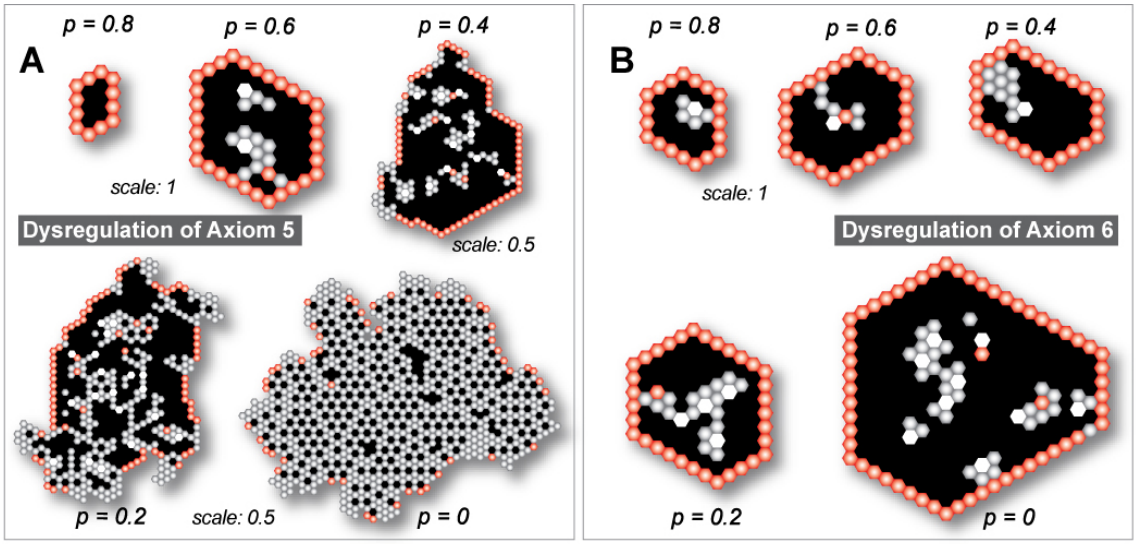

Figure 4.6. Dysregulation of Axiom 5 or 6 has a disruptive effect on ISEA CULTURE morphology in a severity-dependent manner. Axiom 5 dictates ANOIKIS (a form of CELL DEATH) when the CELL in its neighborhood has at least two CELLS and LUMINAL SPACE but no MATRIX. In simulation dysregulating Axiom 5, CELLS evaded ANOIKIS (i.e., do nothing) with a parameter-controlled probability, *p*, when Axiom 5's precondition was met. Axiom 6 dictates oriented CELL DIVISION when the CELL has at least one CELL and MATRIX but no FREE SPACE. When Axiom 6 was dysregulated, CELLS carried out disoriented CELL DIVISION: the CELL copy replaced a randomly selected MATRIX neighbor without regard for CELL neighbor number. Shown are CULTURE images after 50 simulation cycles of growth. Each object is represented as a hexagon: POLARIZED CELL (red), UNPOLARIZED CELL (gray), MATRIX (white), and LUMINAL SPACE (black). (A) Axiom 5 dysregulation caused progressively disorganized CULTURE formations. (B) Axiom 6 dysregulation showed a similarly severity-dependent effect. The changes were less prominent but nevertheless clearly aberrant in both analogues.

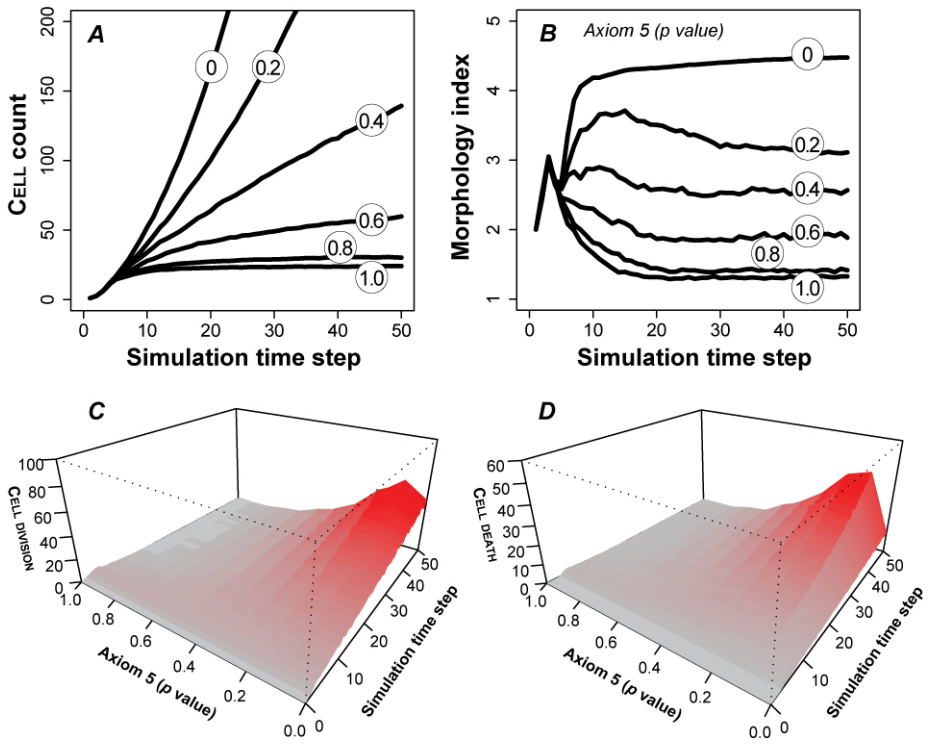

Figure 4.7. Dysregulation of Axiom 5 (ANOIKIS) and its effect on ISEA CULTURE growth and morphology. Axiom 5 dictates CELL DEATH when the CELL has in its neighborhood at least two CELLS and LUMINAL SPACE but no MATRIX. With a parameter-controlled probability, *p*, CELLS evaded ANOIKIS (i.e., do nothing) when Axiom 5's precondition was met. Doing so caused distinct changes in growth and structural characteristics of the EMBEDDED CULTURE. (A) CELL CULTURE growth rate increased monotonically with the severity of dysregulation. CULTURE growths at six levels of dysregulation are shown. (B) Disrupting operation of Axiom 5 resulted in the formation of progressively aberrant MULTICELL structure, as indicated by the numeric scale. Higher values indicate disorganized morphology. Dysregulation had no observable effect on CULTURE morphology in the early stages (~ 5 simulation cycles) of growth. The effect became progressively evident as the simulation time advanced. (C-D) Axiom 5 dysregulation altered CELL DIVISION and DEATH event patterns. The changes became more evident at later time points. In both simulations, the effect on CELL DEATH and DIVISION was monotonic, except for when $p = 0$. The mean occurrence of CELL DIVISION and DEATH fell when $p = 0$ (vs $p = 0.8$). The data represent mean values of 100 Monte Carlo runs.

increased further, depending on the degree of dysregulation. Increased dysregulation always led to a higher mean index value at simulation's end. Images recorded after 50 simulation cycles showed more irregularities and larger structures following increased dysregulation (Fig. 4.6A). The structures exhibited distinctive morphologies depending on dysregulation level. For instance, 'maximal' dysregulation ($p = 0$) resulted in an aggressively expanding CELL mass with minimal POLARIZATION, which failed to develop a central LUMINAL SPACE. The neighborhoods of most CELLS consisted of CELLS and LUMINAL SPACE. On a gross level, the morphological features resembled those associated with in vitro transformation by inhibition of anoikis or apoptosis (Debnath and Brugge, 2005). Less dysregulation resulted in structures in which portions exhibited somewhat normal attributes, including the formation of a central LUMINAL SPACE and increased POLARIZATION along the margins. However, CELLS remained in the LUMINAL SPACE, and most were UNPOLARIZED.

Dysregulation also affected CELL activity patterns. In particular, the number of CELL DEATH and CELL DIVISION occurrences rose steeply over the growth period under severe dysregulation ($p \leq 0.4$), as illustrated in Fig. 4.7C-D. The increase was not as dramatic, and tended to remain relatively steady with less dysregulation. A drop in CELL DIVISIONS was observed when ANOIKIS was abrogated completely ($p = 0$) relative to strong dysregulation ($p = 0.1$). The result was unexpected given the virtually unchecked CULTURE growth measured under that condition. However, even though growth was unchecked, the elimination of ANOIKIS reduced the relative frequency of CELL DIVISION opportunities compared to extensive but incomplete inhibition of Axiom 5 use. Analysis of individual axiom use and their relative frequencies showed that the relative frequency of CELL DIVISION (as a consequence of Axiom 6 use) exceeded the use of all CELL DEATH axioms by a factor of > 2 when $p = 0$. There was a several-fold increase in Axiom 1 activity, but it failed to compensate for the absence of Axiom 5 use; Axiom 2 use showed no observable increase. In partially dysregulated conditions ($p = 0.4–0.8$), Axioms 1 and 2 showed

little activity after the first few simulation cycles. CELL DEATH and DIVISION caused by Axioms 5 and 8 occurred more frequently as simulation progressed, indicative of active PROLIFERATION and DEATH of CELLS in contact with LUMINAL SPACE. Both exhibited similar use frequencies and changes over time.

4.3.4. Axiom 6 dysregulation simulated a disruption in oriented cell division

Oriented cell division is central to multicellular morphogenesis (Sausedo et al., 1997; Gong et al., 2004; Baena-López et al., 2005). Its disruption is implicated in cancer progression (Lee and Vasioukhin, 2008). The cell division axis orientation determines the position of the daughter cells, their contents and hence their fate. It has been shown that both matrix contact and cell adhesions play important roles in determining the orientation of the division axis in vitro (Théry et al., 2005; 2007). What impact would deregulation of oriented cell division have on 3D epithelial cell culture phenotype? If any, could it recapitulate features of early cancer progression? Cell axis and orientation are below the current ISEA resolution. Nevertheless, to the degree that the low granularity mappings in Fig. 4.2 are acceptable, a dysregulated form of Axiom 6, which accounts for most of the CELL DIVISION events that occur during CULTURE growth, can be used to explore plausible answers. To achieve that aim, we dysregulated Axiom 6 by allowing the DIVIDING CELL to place its daughter CELL in a randomly selected MATRIX location (vs one that maximizes CELL contact). We anticipated that, if Axiom 6's operation maps abstractly to a form of oriented cell division in vitro, then the resulting CULTURE phenotype would provide insight into the expected role of oriented cell division in the development, or disruption, of epithelial architecture in vitro.

We ran simulations with Axiom 6's *p* ranging from 0 to 1 and recorded changes in CULTURE growth, morphology, and CELL activity patterns. Some results are shown in Figs. 4.6B and 4.8. CULTURE growth rate increased monotonically with dysregulation (Fig. 4.8A). The changes were less dramatic than those observed when Axiom 5 was dysregulated. With maximal dysregulation,

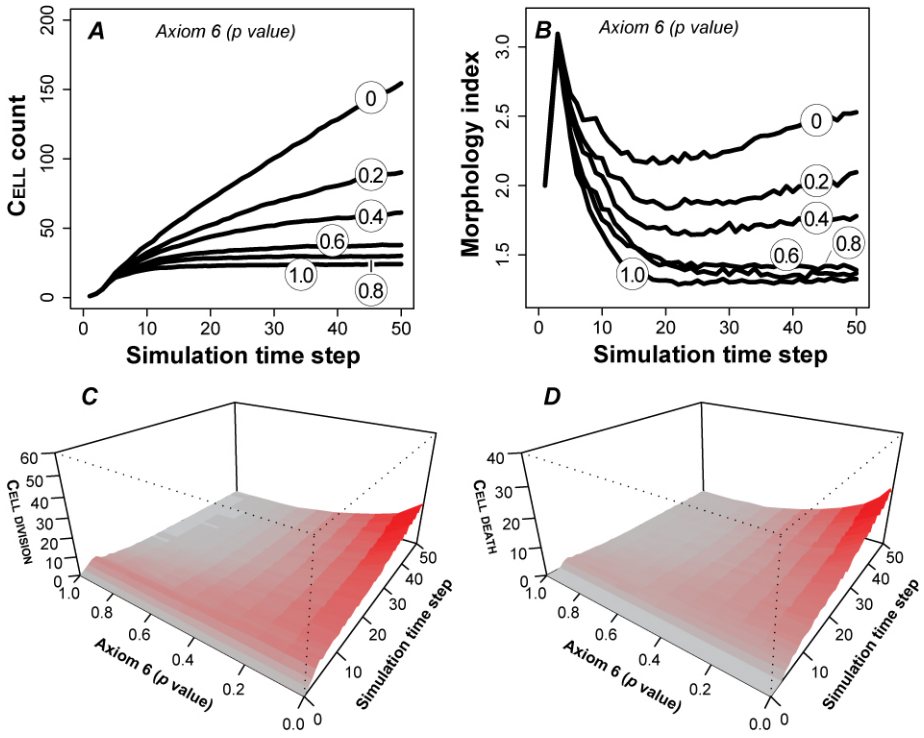

Figure 4.8. Axiom 6 (ORIENTED CELL DIVISION) dysregulation and its effect on ISEA CULTURE growth and morphology. Axiom 6 dictates CELL DIVISION when the CELL has at least one CELL and MATRIX but no FREE SPACE in its neighborhood. The CELL copy is placed at an adjacent MATRIX position that maximizes its number of CELL neighbors. With a parameter-controlled probability, *p*, CELLS followed an alternate, dysregulated action (DISORIENTED CELL DIVISION) when the Axiom 6 precondition was met. The CELL copy replaced a randomly selected MATRIX neighbor without regard for CELL neighbor number. Doing so caused changes in growth and structural characteristics of the EMBEDDED CULTURE. (A) CELL CULTURE growth rate increased monotonically with the severity of dysregulation. (B) Changes in growth morphology. Similar to Axiom 5 dysregulation, the analogue showed no observable effects during the early growth stage but obvious differences over time. (C-D) Axiom 6 dysregulation altered CELL DIVISION and DEATH event patterns. Near the maximally dysregulated state ($p = 0$) showed a proportionately larger increase in CELL DEATH events at later time points. The data represent mean values of 100 Monte Carlo runs.

mean CELL population after 50 simulation cycles reached 150 CELLS, compared with 900 CELLS following Axiom 5 dysregulation. CULTURE morphology also exhibited changes (Fig. 4.8B). When severely dysregulated ($p \leq 0.4$), the developing structures exhibited increasing morphological irregularities. The increase correlated with the presence of UNPOLARIZED CELLS inside the LUMINAL SPACE (Fig. 4.6B). Using CULTURE GUI, we visualized CULTURE growth and observed CELLS undergoing continual, active cycles of PROLIFERATION and DEATH inside the LUMINAL SPACE.

CELL DEATH and DIVISION activities (Fig. 4.8 C-D) continued to register as simulations progressed when highly dysregulated. In fact, the mean number of CELL DIVISIONS and CELL DEATH occurrences increased over time. CELL DEATH events were offset by an approximately equal number of CELL DIVISIONS. Their apparent dynamic balance resembled how a hollow structure is maintained by the increased apoptosis of cells inside the lumen when proliferation is increased in mammary epithelial cell culture (Debnath et al., 2002).

Axiom 6 use accounted for most CELL DIVISION events during early growth (not shown), but in a more severely dysregulated state, Axiom 8 (another driver of CELL DIVISION) was used more frequently as simulation progressed. The increase in CELL DIVISION was offset by a similar increase in Axiom 5 (ANOIKIS) use frequency. Decreased use of Axiom 12 (do nothing) provided further evidence for the continual, dynamic CELL turnover occurring inside the LUMINAL SPACE during growth. That is because current ISEA axiom use assumes that nutrient availability is the same in LUMEN as in the EXTRACELLULAR CULTURE. If that is not the case, then it is straightforward to make axiom use frequencies nutrient dependent.

4.3.5. Dysregulation of ANOIKIS and ORIENTED CELL DIVISION

We also explored conditions in which Axioms 5 and 6 were dysregulated simultaneously. The experiments may map to experimental manipulation of protein complexes such as activated receptor tyrosine kinases in epithelial cell culture, which can deregulate both cell division and cell

death processes (Debnath and Brugge, 2005). We varied the two axioms' *p* independent of each other and conducted 100 Monte Carlo simulation experiments for each condition. The dysregulated ISEA, illustrated in Fig. 4.9, exhibited nonlinear growth changes. Change was most striking for the maximally dysregulated condition ($p = 0$), which resulted in a mean CELL population of ~ 2000 CELLS vs ~ 900 CELLS when only Axiom 5 was dysregulated, or 150 CELLS from deregulating only Axiom 6. Changes at other tested levels were also nonlinear (Fig. 4.9A). As measured by CELL count and morphology index (Fig. 4.9A, B), Axiom 5 dysregulation contributed more to observed phenotypic changes. When Axiom 5 was maximally dysregulated, ISEA produced structures with morphology index values > 4, regardless of Axiom 6's *p* (Fig. 4.9B). Simulation images (Fig. 4.9C) recorded after 50 simulation cycles showed differentiable morphologies that roughly coincided with different gradations observed in Fig. 4.9B. The altered ISEA morphologies mapped to characteristics of the in vitro cancer reconstruction model and early cancer progression in vivo (Tlsty et al., 2004; Debnath and Brugge, 2005; Hebner et al., 2008).

Results from the above experiments, we observed similar morphologies regardless of which axiom was dysregulated. No new features emerged from simultaneous dysregulation of Axioms 5 and 6. For example, note the CULTURE images in Figs. 4.6A ($p = 0.6$), 4.6B ($p = 0.2$), and 9C (Axiom 5's $p = 0.8$ and Axiom 6's $p = 0.4$). The similar features included formation of a central LUMINAL SPACE, which is fully enclosed by a monolayer of POLARIZED CELLS, and the presence of mostly UNPOLARIZED CELLS in the inner region. The similarities were reflected in the morphology index measurements. Consequently, we could not infer from CULTURE morphology alone which axiom (Axiom 5, 6, or both) had been dysregulated. However, making such a determination is straightforward given CELL axiom use patterns. In time, gene or protein expression patterns of individual cells may emerge as the wet-lab counterpart to axiom use patterns.

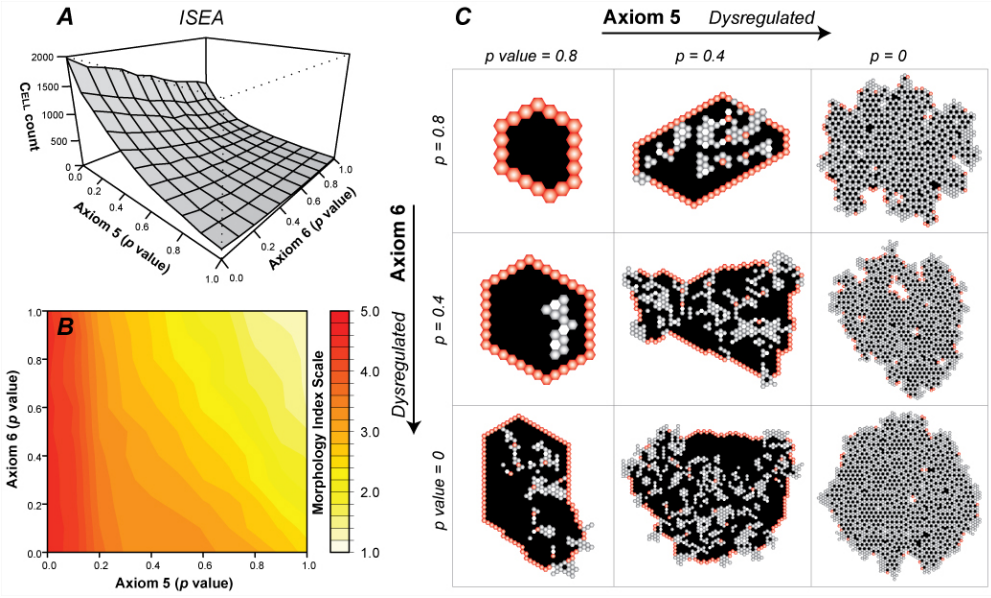

Figure 4.9. Simultaneous dysregulation of Axioms 5 and 6 and its effect on ISEA CULTURE growth and morphology. Axioms 5 and 6 dictate ANOIKIS (a form of CELL DEATH) and ORIENTED CELL DIVISION; both are essential to normal CYST growth in EMBEDDED culture. With a parameter-controlled probability, *p*, for each of the two axioms, CELLS followed an alternate, dysregulated action. For Axiom 5, the alternate action was to evade ANOIKIS (i.e., do nothing). For Axiom 6, it was disoriented CELL DIVISION; the CELL copy replaces a randomly selected MATRIX neighbor. (A) ISEA CELL population, (B) morphology index values, and (C) simulation images after 50 simulation cycles of growth. Each object is represented as a hexagon: POLARIZED CELL (red), UNPOLARIZED CELL (gray), MATRIX (white), and LUMINAL SPACE (black). The CELL count and morphology measurements represent mean values of 100 Monte Carlo runs.

4.4. Discussion

Studies of epithelial cell cultures are providing knowledge about how individual cell activities are mediated by intrinsic and environmental factors to create the diverse phenotypes of normal epithelial morphogenesis and epithelial cancers. There is a need for additional methods to facilitate a deeper, integrated understanding of the growing body of experimental observations. Past efforts have demonstrated how combined experimental and computational approaches contribute to that process (Kitano, 2002; Aloy and Russell, 2006). Our goal is to broaden and strengthen that effort by developing software analogues that are useful 1) as instantiated, working hypotheses of epithelial morphogenesis and tumorigenic phenotype in vitro, and 2) as an extensible, interactive resource of available biological knowledge about the mechanisms implicated in those processes. Progress described herein represents an early step towards achieving those goals.

We revised and extended the axiomatic operating principles of an earlier model (Grant et al., 2006) to those shown in Fig. 4.4. The revised ISEA consistently produced roundish, convex CYSTS with smooth margins, a cardinal feature of normal in vitro MDCK phenotype. We enabled mechanistic tracing during simulations of all processes essential for normal ISEA development. Two critical axioms were targeted for dysregulation: Axiom 5, which controlled ANOIKIS, and Axiom 6 that dictated an abstract form of oriented cell division. The causal chains of events responsible for ISEA phenotype were explored in detail following dysregulation, a process which is infeasible using current state-of-the-art in vitro methods.

Dysregulated ISEA phenotypes exhibited features reminiscent of those associated with in vitro cancer reconstruction models and early cancer progression in vivo. By increasing dysregulation of the two axioms, we altered ISEA phenotype progressively to mimic features of epigenetic change that accompany early precursor lesions like atypical ductal hyperplasia (Tlsty et al., 2004). ISEAs using dysregulated ANOIKIS (Axiom 5) developed MULTICELLULAR

structures having ill-formed LUMINAL SPACES containing disorganized nests of CELLS. With increased dysregulation, LUMINAL CELLS sometimes broke out through the enclosing monolayer to PROLIFERATE into the surrounding MATRIX, as illustrated in Fig. 4.9C. Although such behavior has not been observed in studies of apoptosis inhibition in 3D culture, the activation of certain growth factor receptors able to promote luminal space survival, such as ErbB2, do exhibit similar expansive phenotypes in 3D (Muthuswamy et al., 2001; Debnath et al., 2002). If a mapping does exist between those ISEA behaviors and phenomena of epithelial systems, it suggests that epigenetic changes may be capable of inducing invasive behaviors in otherwise apparently normal cells in vitro or in vivo (Tlsty et al., 2004; Rizki et al., 2008). The phenomena merits further in silico exploration.

Similar, but less dramatic changes were observed when we dysregulated oriented CELL DIVISION (Axiom 6). Simultaneous dysregulation of the two axioms produced nonadditive effects but no new morphological features emerged: the structures were virtually indistinguishable from those obtained by dysregulating only Axiom 5 or 6. Consequently, without a priori dysregulation knowledge, one would be unable to reliably deduce the operational cause of a change in CULTURE phenotype based solely on morphology images. A similar conclusion has been reached based on in vitro findings that phenotypic changes such as lumen filling in 3D cultures can be induced by deregulation of different molecular mechanisms (Debnath and Brugge, 2005). To the extent that the in silico-to-in vitro and in vitro-to-in vivo mappings are valid, the results support the idea that morphologically similar dysplasia can have different causes, and that may have implications for early diagnosis of cancer based on morphology alone, as very aggressive, early stage cancers may appear morphologically similar to potentially less aggressive, abnormal, non-cancerous growths.

Dysregulation of either axiom enabled some CELLS to survive in the LUMINAL SPACE. That ISEA behavior maps to in vitro observations (Debnath and Brugge, 2005; Hebner et al., 2008). How the latter occurs has not been determined. How it occurs within ISEA may provide insight.

In simulations, a subset of INTRALUMINAL CELLS established MATRIX contact by producing MATRIX de novo (via Axiom 4 use). So doing enabled them and some other CELLS to survive in aggregates inside the LUMINAL SPACE, where they underwent cycles of PROLIFERATION and DEATH. Blocking the CELLS' ability to produce MATRIX (Axiom 4) reduced INTRALUMINAL CELL survival dramatically, and facilitated clearing of residual INTRALUMINAL CELLS during LUMINAL development (data not shown). In vitro, similar phenomena have been observed in MCF-10A epithelial cell cultures: cells accumulated inside cyst lumens when an antiapoptotic protein, Bcl-2 was overexpressed (Debnath et al., 2002). However, unlike in ISEA simulation, the cells eventually died and disappeared. Mechanisms underlying the latter process are unknown. Interestingly, some evidence suggests that Bcl-2 activates matrix metalloproteinase (MMP), which degrades ECM surrounding cells (Choi et al., 2005). Do the above INTRALUMINAL CELL survival observations have an in vitro counterpart, or are these ISEA behaviors outside the area of phenotype overlap illustrated in Fig. 4.1? If there is an in vitro counterpart, then intraluminal epithelial cells in 3D embedded culture may evade apoptosis and further insure their survival by secreting matrix de novo for anchorage. In such a scenario, MMP activation could have an opposing effect by degrading the cell-secreted matrix, rendering the cells vulnerable to anchorage-dependent anoikis.

Dysregulation of Axiom 6 demonstrated the importance of proper DIVISION direction during CULTURE growth. Evidence supports a mapping to in vitro counterparts. Similar structures form when cell polarity is disrupted in MDCK cell cultures by ablating the mammalian ortholog of PALS1, a gene involved in epithelial polarity in Drosophila (Straight et al., 2004). Similar to ISEA behaviors, the structures contain multiple intraluminal cell clusters and resemble certain patterns observed in breast ductal carcinomas in situ and prostate hyperplasia (Hebner et al., 2008). Because cell polarity is critical to cell division orientation, one could speculate that a disruption in oriented cell division by PALS1 ablation may have contributed to the observed

phenomenon. We also note that several groups have discovered that Ric-8 protein plays a key part in the positioning of the division axis in Drosophila morphogenesis (David et al., 2005; Wang et al., 2005). It is not yet known if Ric-8 plays a similar role in oriented mammalian cell division in cultures. Nevertheless, ISEA behaviors indicate that compromising one or more of the mechanisms managing oriented epithelial cell division can contribute to features of early stage, cancer-like structures in 3D cultures.

The ISEA methods used to mimic attributes of cancer reconstruction differ from those used to model tumor growth in vitro and in vivo. Recent models (Anderson et al., 2006; Schaller and Meyer-Hermann, 2006; Harpold et al., 2007; Wang et al., 2007; Engelberg et al., 2008) have represented cancerous cells as permanently transformed cell line. We explored incremental dysregulation of specific ISEA mechanisms. Galle et al. (2005) used a similar, creative, individual cell-based approach to simulate and study epithelial cell monolayer growth. They used selective "knockouts" of cell level growth regulation and control mechanisms to investigate how those different mechanisms collectively acted together to influence population morphology.

CELL axioms are high level, low-resolution placeholders for more detailed representations of the actual complex mechanisms driving epithelial cell behavior. Use of axioms precludes explicit representations of the abundant, detailed subcellular information that is available. However, starting with the current more abstract set of axioms provided the simplest method and approach for building a useful, working model, positing principles of operation, and testing hypotheses as discussed above. On the other hand, a key advantage of the approach built into ISEA and framework designs are their adaptability for inclusion of additional attributes and details through an iterative model refinement process. The current analogue and its components, including CELL axioms, can be further developed to reflect new biological information (e.g., cell positioning mechanisms). We can elaborate ISEA to include higher granularity components and mechanisms that map to subcellular details such as cell lifecycle pathways and intercellular signaling networks

when validation against an expanded set of targeted attributes requires doing so. From an engineering perspective, doing so is straightforward and can be accomplished by swapping the current component (e.g., CELL) for a more detailed composite agent. Replacement could also occur at the intra-component level, for example by replacing CELL axioms with more detailed logic based on interacting components. By so doing we can strengthen the in silico-to-in vitro mappings illustrated in Fig. 4.2. A challenging task will be to insure cross-model validation between the different analogue variants, and develop appropriate automated validation measures.

In summary, the approach described herein enabled instantiating a working hypothesis of how individual epithelial cell actions may give rise to cyst organization in vitro, and when disrupted selectively, to structures having tumor-like characteristics. Modest dysregulation of one of two key ISEA operating principles was sufficient to cause manifest changes in its original phenotype. The results support the position that epigenetic deregulation of cell principles of operation is sufficient to cause emergence of attributes of early stage cancers. We anticipate future rounds of ISEA refinement and validation will further strengthen each of the mappings in Fig. 4.2, and provide an additional, viable experimental approach to dissect the operational basis of glandular epithelial morphogenesis and cancer progression.

References

1. Aloy P, Russell RB (2006) Structural systems biology: modelling protein interactions. *Nat Rev Mol Cell Biol* 7:188-197.
2. Anderson AR, Weaver AM, Cummings PT, Quaranta V (2006) Tumor morphology and phenotypic evolution driven by selective pressure from the microenvironment. *Cell* 127:905-915.
3. Baena-López LA, Baonza A, García-Bellido A (2005) The orientation of cell divisions determines the shape of Drosophila organs. *Curr Biol* 15:1640-1644.
4. Boudreau N, Sympson CJ, Werb Z, Bissell MJ (1995) Suppression of ICE and apoptosis in mammary epithelial cells by extracellular matrix. *Science* 267:891-893.
5. Choi J, Choi K, Benveniste EN, Rho SB, Hong YS, Lee JH, Kim J, Park K (2005) Bcl-2 promotes invasion and lung metastasis by inducing matrix metalloproteinase-2. *Cancer Res* 65:5554-5560.

6. David NB, Martin CA, Segalen M, Rosenfeld F, Schweisguth F, Bellaïche Y (2005) Drosophila Ric-8 regulates Galphai cortical localization to promote Galphai-dependent planar orientation of the mitotic spindle during asymmetric cell division. *Nat Cell Biol* 7:1083-1090.
7. Debnath J, Mills KR, Collins NL, Reginato MJ, Muthuswamy SK, Brugge JS (2002) The role of apoptosis in creating and maintaining luminal space within normal and oncogene-expressing mammary acini. *Cell* 111:29-40.
8. Debnath J, Brugge JS (2005) Modelling glandular epithelial cancers in three-dimensional cultures. *Nat Rev Cancer* 5:675-688.
9. Engelberg JA, Ropella GE, Hunt CA (2008) Essential operating principles for tumor spheroid growth. *BMC Syst Biol* 2:110.
10. Fisher J, Henzinger TA (2007) Executable cell biology. *Nat Biotechnol* 25:1239-1249.
11. Galle J, Loeffler M, Drasdo D (2005) Modeling the effect of deregulated proliferation and apoptosis on the growth dynamics of epithelial cell populations in vitro. *Biophys J* 88:62-75.
12. Gong Y, Mo C, Fraser SE (2004) Planar cell polarity signalling controls cell division orientation during zebrafish gastrulation. *Nature* 430:689-693.
13. Grant MR, Mostov KE, Tlsty TD, Hunt CA (2006) Simulating properties of in vitro epithelial cell morphogenesis. *PLoS Comput Biol* 2:e129.
14. Grimm V, Revilla E, Berger U, Jeltsch F, Mooij WM, Railsback SF, Thulke HH, Weiner J, Wiegand T, DeAngelis DL (2005) Pattern-oriented modeling of agent-based complex systems: lessons from ecology. *Science* 310:987-991.
15. Harpold HL, Alvord EC Jr, Swanson KR (2007) The evolution of mathematical modeling of glioma proliferation and invasion. *J Neuropathol Exp Neurol* 66:1-9.
16. Hebner C, Weaver VM, Debnath J (2008) Modeling morphogenesis and oncogenesis in three-dimensional breast epithelial cultures. *Annu Rev Pathol Mech Dis* 3:313-339.
17. Hunt CA, Ropella GE, Park S, Engelberg JA (2008) Dichotomies between computational and mathematical models. *Nat Biotechnol* 26:737-738.
18. Kitano H (2002) Systems biology: a brief overview. *Science* 295:1662-1664.
19. Law AM, Kelton WD (2000) *Simulation modeling and analysis.* New York: McGraw-Hill.
20. Lee M, Vasioukhin V (2008) Cell polarity and cancer--cell and tissue polarity as a non-canonical tumor suppressor. *J Cell Sci* 121:1141-1150.
21. Martín-Belmonte F, Yu W, Rodríguez-Fraticelli AE, Ewald AJ, Werb Z, Alonso MA, Mostov K (2008) Cell-polarity dynamics controls the mechanism of lumen formation in epithelial morphogenesis. *Curr Biol* 18:507-513.
22. Montesano R, Schaller G, Orci L (1991) Induction of epithelial tubular morphogenesis in vitro by fibroblast-derived soluble factors. *Cell* 66:697-711.
23. Muthuswamy SK, Li D, Lelievre S, Bissell MJ, Brugge JS (2001) ErbB2, but not ErbB1, reinitiates proliferation and induces luminal repopulation in epithelial acini. *Nat Cell Biol* 3:785-792.

24. O'Brien LE, Zegers MM, Mostov KE (2002) Building epithelial architecture: insights from three-dimensional culture models. *Nat Rev Mol Cell Biol* 3:531-537.
25. Rizki A, Weaver VM, Lee SY, Rozenberg GI, Chin K, Myers CA, Bascom JL, Mott JD, Semeiks JR, Grate LR, Mian IS, Borowsky AD, Jensen RA, Idowu MO, Chen F, Chen DJ, Petersen OW, Gray JW, Bissell MJ (2008) A human breast cell model of preinvasive to invasive transition. *Cancer Res* 68:1378-1387.
26. Sausedo RA, Smith JL, Schoenwolf GC (1997) Role of nonrandomly oriented cell division in shaping and bending of the neural plate. *J Comp Neurol* 381:473-488.
27. Schaller G, Meyer-Hermann M (2006) Continuum versus discrete model: a comparison for multicellular tumour spheroids. *Philos Transact A Math Phys Eng Sci* 364:1443-1464.
28. Straight SW, Shin K, Fogg VC, Fan S, Liu CJ, Roh M, Margolis B (2004) Loss of PALS1 expression leads to tight junction and polarity defects. *Mol Biol Cell* 15:1981-1990.
29. Théry M, Racine V, Pépin A, Piel M, Chen Y, Sibarita JB, Bornens M (2005) The extracellular matrix guides the orientation of the cell division axis. *Nat Cell Biol* 7:947-953.
30. Théry M, Jiménez-Dalmaroni A, Racine V, Bornens M, Jülicher F (2007) Experimental and theoretical study of mitotic spindle orientation. *Nature* 447:493-496.
31. Tlsty TD, Crawford YG, Holst CR, Fordyce CA, Zhang J, McDermott K, Kozakiewicz K, Gauthier ML (2004) Genetic and epigenetic changes in mammary epithelial cells may mimic early events in carcinogenesis. *J Mammary Gland Biol Neoplasia* 9:263-274.
32. Wang H, Ng KH, Qian H, Siderovski DP, Chia W, Yu F (2005) Ric-8 controls Drosophila neural progenitor asymmetric division by regulating heterotrimeric G proteins. *Nat Cell Biol* 7:1091-1098.
33. Wang Z, Zhang L, Sagotsky J, Deisboeck TS (2007) Simulating non-small cell lung cancer with a multiscale agent-based model. *Theor Biol Med Model* 4:50.
34. Yu W, Datta A, Leroy P, O'Brien LE, Mak G, Jou TS, Matlin KS, Mostov KE, Zegers MM (2005) β1-integrin orients epithelial polarity via Rac1 and laminin. *Mol Biol Cell* 16:433-445.
35. Zeigler BP, Kim TG, Praehofer H (2000) Theory of modeling and simulation: integrating discrete event and continuous complex dynamic systems. San Diego: Academic Press.